RSC Advances

ROYAL SOCIETY OF CHEMISTRY

www.rsc.org/advances

The plasticized spinning and cyclization behaviors of functionalized carbon nanotube/polyacrylonitrile fibers

Xiang Li, Xiaofei Ji, Aiwen Qin, Chunju He*
State Key Lab for Modification of Chemical Fibers and Polymer Materials
College of Material Science & Engineering
Donghua University
Shanghai 201620 (P. R. China)

Abstract

The plasticized spinning and cyclization behaviors of polyacrylonitrile (PAN) and polyacrylonitrile/functionalized carbon nanotube (PAN/CNT-COOH) composite fibers were studied. The PAN/CNT-COOH fibers containing 0.8wt.% CNTs exhibit excellent tensile strength and modulus, i.e. 0.475GPa and 10.93 GPa, which are 69.6% and 40.13% improvement respectively, comparing to their precursor fibers. The changing trend of crystallinity of PAN/CNT-COOH fibers is associated with the heat exchange rate and oriented-crystallization rate, which can be confirmed by the X-ray diffraction (XRD) results. The cyclization behaviors of the fibers were examined using X-ray photoelectron spectrometer (XPS), differential scanning calorimeter (DSC) and X-ray diffraction (XRD). The results show that cyclization of PAN/CNT-COOH fibers are initiated by three types of initiating agents, i.e., modified CNTs (CNTs-COOH), oxygen containing groups generated during the plasticized spinning and comonomers. Meanwhile, the PAN/CNT-COOH fibers exhibit various cyclization behaviors induced by high spinning speed.

* Corresponding authors: Fax: +86-021-6779 2855.
E-mail: chunjuhe@dhu.edu.cn (C.J. He)
Tel: +86-021-6779 2842

1. Introduction

In recent decades, carbon fibers (CFs) have been widely utilized as a reinforcement for high-strength composites due to their high strength-to-weight ratio and superior stiffness [1,2]. Nowadays, polyacrylonitrile (PAN) based CFs have dominated nearly 90% of all the carbon consumption in the world [3]. Currently, a few percentages of carbon nanotubes (CNTs) are incorporated to PAN matrix to improve the mechanical properties of resulting fibers since CNTs have been considered as the excellent reinforcement for polymer [4-7]. The PAN/CNT fibers are frequently fabricated through the wet spinning process, the utilize of the polar solvents, e.g. dimethylacetamide [8,9] and dimethylformamide [10,11], leads to structural defects, low production efficiency, environmental pollution, health problems and so on.

Nowadays, external plasticization of PAN/CNT system has obtained lots of attention due to its high efficiency and low consumption of organic solvents. The introduction of plasticizes to PAN matrix leads to decrease in glass transition temperature and melting point, elastic modulus and so on[12,13]. Recent reports about using Ethylene carbonate (EC) as a plasticizer for PAN/CNT system [14,15] to achieve the plasticized spinning of PAN/CNT fibers. However, the reported values of mechanical strength of PAN/CNT fibers are far below the predictions, due to the low polarity and thermal instability of EC, and agglomeration of the CNTs induced by simple blending, giving rise to poor structure and large diameter i.e. 250μm of the resulting fibers. Meanwhile, the conformational evolution and phase transition of the PAN/CNT fibers caused by spinning speed has not been systematically studied. Such a situation raises a critical demand for the researchers in the field to look for an alternative plasticizer, which is also capable of improving the structures and mechanical properties of the

fibers without occurrence of these problems. In our recent study [16], we have proved that 1-butyl-3-methylimidazolium chloride ([Bmim]Cl) can be employed as a excellent plasticizer for PAN due to its high polarity and thermal stability.

In addition, it is worthy noted that the quality of CFs is strongly dependent on the stabilization [17], which contains various chemical reactions, i.e., cyclization, oxidation and dehydrogenation [18,19]. And cyclization is considered to be the most important reactions [20-22] since another two reactions only occur in cyclized fibers [23]. The fast cyclization reaction and high heat released (ΔH) result in poor mechanical properties and imperfect structure of the fibers[24]. Consequently, slow cyclization reaction and low ΔH improve the performances of the CFs. Therefore, it is very important to study the cyclization behaviors of the PAN/CNT-COOH fibers to provide a better understanding on conformational changes of the fibers during the cyclization process and furnish important information for the development of CFs.

In this research, the plasticized spinning of PAN/CNT-COOH fibers was successfully achieved, the fibers exhibit high strength than PAN fibers. To the best of our knowledge, we have not identified any previous literature to report about the plasticized spinning of PAN/CNT-COOH fibers. Moreover, it is found that the crystallinity of the fibers is closely related to heat exchange rate and oriented-crystallization rate. Finally, the addition of CNT-COOH to PAN fibers reduce the initiation temperature for cyclization and ΔH of the fibers, which contributes to cyclization.

2. Experimental section

2.1 Materials

1-chlorobutane and N-methylimidazole were purchased from Sinopharm Chemical Reagent Co, Ltd.. PAN copolymer powder ($M\eta=1.5\times10^5$g/mol, acrylonitrile/methylacrylate/acrylamide= 97.5/2.2/0.3 mol%) was also synthesized in our laboratory. Pristine multi wall carbon nanotubes (length:1-5μm, diameter: 40-50nm, nominal purity>97%) were purchased from Shenzhen Nanotech Port Corporation Limited. To enhance the compatibility with the polymer, the CNTs were oxidized by a concentrated H_2SO_4/HNO_3 mixture (3:1) solution. The oxidation process was conducted according to the reference [25], then the surface-oxidized CNTs (CNTs-COOH) were filtered with microfiltration membranes (pore size 0.2 μm, polytetrafluoroethylene). The CNTs were rinsed repeatedly with deionized water until acid free, dried in a vacuum oven at 60ºC for 48h.

2.2 Preparation of samples

The surface-oxidized CNTs (CNTs-COOH) are apt to aggregate after drying in an oven due to the high van der Waals forces. It is very hard to disperse the lump CNTs-COOH (in Fig. 1 a) in plasticizer due to its high viscosity. In order to better disperse the surface-oxidized CNTs, in-suit synthesis method was adopted, that is CNTs-COOH was mixed with 0.105mol 1-chlorobutane and 0.095mol N-methylimidazole in a flask followed by sonication for 2h. The mixture was conducted at 80ºC with magnetic stirring under a nitrogen atmosphere. After 48h reaction, the [Bmim]Cl (PL) /CNT-COOH system was got (in Fig. 1 b). The same PL/CNT-COOH system was fabricated by blending. 1-chlorobutane and N-methylimidazole

with a molar ratio of 1:0.9 were also conducted in a flask at 80ºC for 48h under continuous magnetic stirring, finally the PL was obtained. All systems were washed using ethyl acetate for three times, then dried under vacuum at 80ºC to remove the volatile solvent residue. The prepared PL/CNT-COOH and PL were mixed with 75g of PAN powder respectively under a liquid nitrogen to ensure the blending homogeneity.

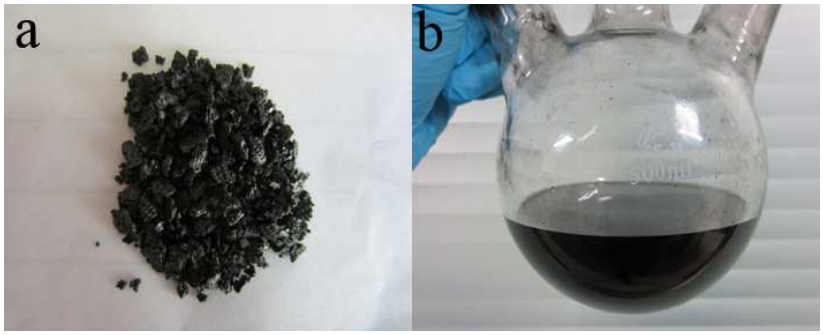

Fig. 1. The dispersion process of lump CNTs-COOH in 1-chlorobutane and N-methylimidazole system: (a) the lump CNTs-COOH; (b) the [Bmim]Cl/CNT-COOH system.

2.3 Plasticized spinning of PAN and PAN/CNT fibers

The PAN, PAN/CNT and PAN/CNT-COOH composite fibers were prepared under a condition of constant temperature (20°C±1°C) and humidity (20%±1°C) to ensure the reproducibility of the experimental results. The plasticized spinning process was conducted at the spinning speeds of about 30m/min, 40m/min and 50m/min,the fibers were fabricated via a self-made extruder [16]. Feeding quality of the extruder in one minute was constant, a smaller diameter of the fibers indicated a higher spinning speed was utilized. The as-spun fibers were collected using a coiler. Then the prepared fibers were washed by deionized water to remove the remaining PL and dried in an oven at 70ºC for 48h.

2.4 Measurements

Transmission electron microscopy (TEM, JEM-2100, JEOL, Japan) was utilized to

examine structure of the CNTs-COOH. A certain amount of CNTs-COOH were dispersed in Methanol followed ultrasonic dispersion for 5min, then TEM observation was conducted.

The Infrared spectra (IR) spectrum was recorded using a FTIR (Spectrum BX□, Perkin Elmer, US) spectrometer in the range of 400-4000cm^{-1} using KBr pellets.

Raman spectroscopy (inVia-Reflex, Renishaw, UK) was employed to investigate the chemical bandings of the fibers. The measurements are performed using 633 nm excitation laser at room temperature.

Optical microscope (59XD, Shanghai optical instrument factory, China) was utilized to observe the morphological structures the fibers.

Scanning electron microscopy (SEM, S-4800, HITACHI, Japan) was used to observe the cross-section of the fibers.

X-ray photoelectron spectrometer (XPS, AXIS ULTRA DLD, Japan) was used to determine the surface chemical composition of the composite fibers. Al Kα (1486.6 eV) was used as a the X-ray source, the takeoff angle of photoelectron radiation was set at 90°.

Differential scanning calorimeter (Q20, TA, US) was used to determine the thermal performance of fibers under the nitrogen atmosphere, the fibers were cut into pieces and 2mg fibers were employed. The heating rate was 10ºC/min and the fibers were heated from room temperature to 400 ºC.

The X-ray diffraction analysis (XRD) using CuKα (λ=0.1542 nm) for composite fibers was conducted under the X-ray diffractometer (D/Max-2550 PC, RIGAKU, Japan), the operation voltage and electricity were 30kv and 10mA respectively. The average crystal size (Lc) was calculated according to the Scherrer equation[26]:

$$L_C = \frac{k\lambda}{\beta\cos\theta} \quad (1)$$

where K is a constant, which was taken to be 0.89; λ=0.1542 nm is the wavelength of the X-rays; β is the full width at half maximum in radians at 2θ =17°.

The crystallinity was determined from the XRD patterns of the fibers according to the formula calculated by Hinrichsen's method [27]:

$$C\% = \frac{Ac}{Ac + Aa} \quad (2)$$

where Ac is the integral area of the crystalline region, and Aa is the integral area of the amorphous region.

The orientation in crystalline of the fibers was measured by XRD diffraction, the fibers was scanned around 2θ =17°. and the degree of orientation was determined by the following equation [28]:

$$\pi(\%) = \frac{180 - H}{180} \times 100\% \quad (3)$$

where H is the full width at half the maximum intensity at 2θ=17° diffraction.

Peakfit soft (v4.12) was utilized for peak fitting of XRD spectra in the range of 20°-50°.

The fiber tensile strength machine (XQ-1, Shanghai New Fiber Instrument Co., Ltd., China) was used to measure the mechanical properties of PAN fibers at a gauge length of 20mm and at a cross-head speed of 20mm/min.

3. Results and discussion

3.1 Characterization of functionalized CNTs

The morphologies of pristine and carboxylic (-COOH) CNTs can be seen in Fig. 2. The

CNTs-COOH were much shorter than the original ones due to the modification. The CNTs-COOH had rougher walls and open ends [29], modification of the CNTs also can be confirmed by FTIR and Raman spectra.

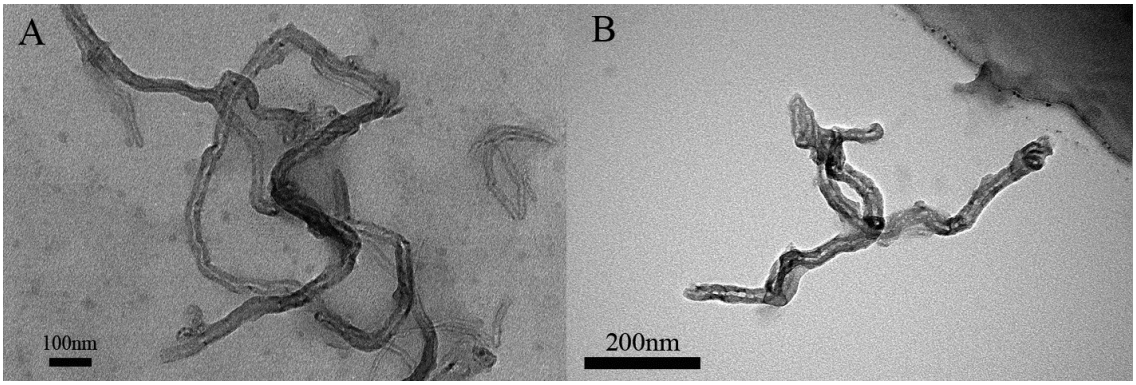

Fig. 2. TEM pictures of pristine CNTs (A) and carboxyl-functionalized CNTs (B).

As can be seen Fig. 3 a, the FTIR spectrum of the pristine CNTs basically do not show any characteristic peaks. The FTIR spectrum of CNTs-COOH exhibits characteristic peaks of OH at 3426.6cm^{-1}, CH at 2962.6, 2953.6 and 2851.2 cm^{-1}, C=O at 1719.1 and 1633.62cm^{-1}, indicating the appearance of the C=O grafted on CNTs.

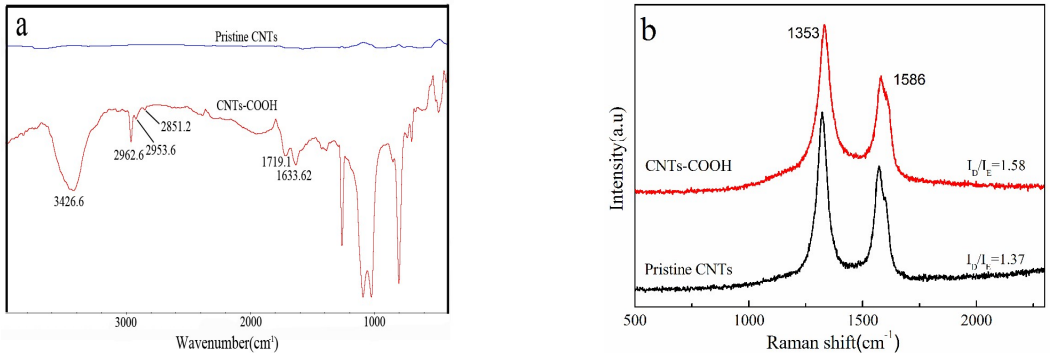

Fig. 3. FTIR spectra (a) and Raman spectra (b) of pristine CNTs and functionalized CNTs

In Fig. 3 b, both pristine CNTs and CNTs-COOH show two strong bands, the G-band at around 1586 cm^{-1} and the D-band at around 1353 cm^{-1}. The D-band corresponds to the defects on the CNTs, whereas the G-band is due to the order carbon [30]. It is calculated that the area ratio of D-band to G-band intensity (D/G ratio) of pristine CNTs is about 1.37, while

the D/G ratio of CNTs-COOH is increased to 1.58, confirming the formation of defects site on the CNTs induced by modification.

3.2 The interactions among the PAN, PL and CNTs-COOH

The interactions among the PAN, PL and CNTs-COOH can be seen in Fig. 4. After heating at 160ºC for 5 min, C≡N vibration bands of PAN powder are observed at 2242.92cm^{-1} and the C-H bands of imidazolium rings in PL are shown at 3132.52cm^{-1} [31,32] (in Fig. 4 a). The position of C≡N groups is red-shifted to 2239.55cm^{-1} in PAN/PL system, meanwhile, the C-H bands of imidazolium rings are blue-shifted to 3146.11cm^{-1}. In our recent study [14], it has been discussed that the interaction belongs to hydrogen bonding (C-H···N).

As can be seen in Fig. 4 (b), the position of C-H bands of imidazolium rings is blue-shifted to 3150.89 cm^{-1} in PAN/PL/CNT-COOH system**,** suggesting the formation of the interaction between CNTs-COOH and PL through the "cation-π" interaction [33,34]. It is worthy noted that the plasticizing process is accompanied with the formation of strong interaction between PAN and plasticizer, and the weakness in interaction between C≡N groups, which can be confirmed by the movement of the C≡N groups in FTIR spectra. It is believed that a better plasticizing effect implies a greater red shift of C≡N bands [16]. Consequently, compared with PAN/IL system, the position of the C≡N groups is basically not shifted for PAN/PL/CNT-COOH system, revealing that the plasticizing effect is not affected as the CNT-COOH are incorporated.

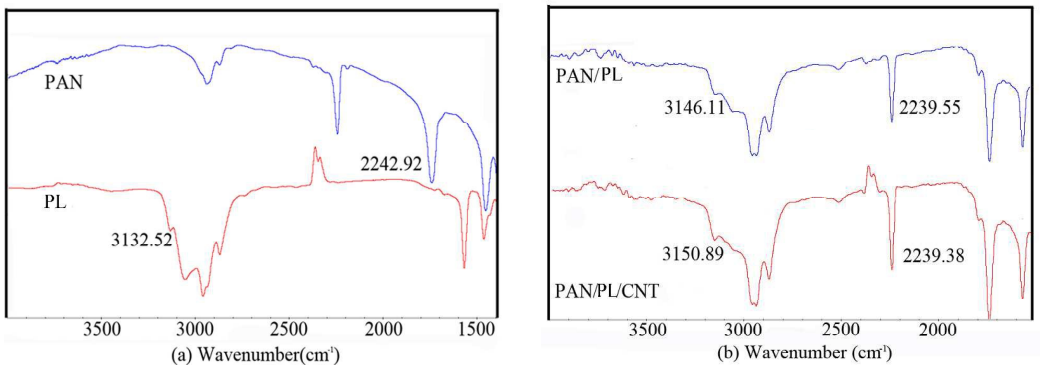

Fig. 4. The FTIR spectra of PAN, PL, PAN/PL and PAN/PL/CNT-COOH at 160ºC temperature.

3.3 Morphological structures of the PAN/CNT composite fibers

Fig. 5 shows the optical micrographs of the PAN/CNT-COOH composite fibers. The diameter of all fibers is in the range of 27-34μm, it is worthy noted that the post drawing has not been utilized in this paper.

A large number of black particles can be observed in the PAN/CNT-COOH fibers prepared by blending, suggesting the agglomeration of CNTs-COOH. However, it is hard to observe black particles in the PAN/CNT-COOH fibers fabricated by in-suit synthesis even at the high CNTs-COOH content, i.e. 1.2wt.%, indicating that the CNTs-COOH are dispersed well in the PAN /CNT-COOH fibers.

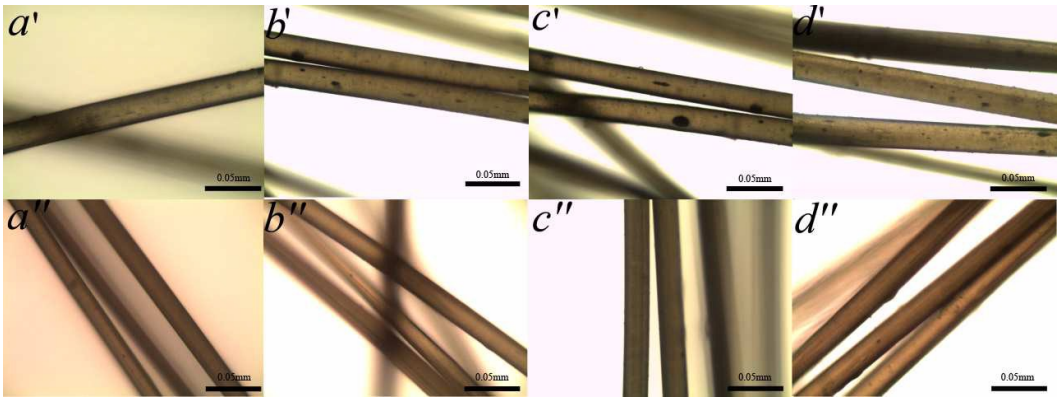

Fig. 5. Optical micrographs of PAN/CNT-COOH (blending) and PAN/CNT-COOH (in-suit synthesis) fibers: a'and a''. 0.5wt.% CNTs-COOH ; b' and b'' 0.8wt.% CNTs-COOH ; c' and c'' 1wt.% CNTs-COOH ; d' and d'' 1.2wt.% CNTs-COOH .

The scanning electron microscopy (SEM) images of the fibers can be seen in Fig. 6,

both fibers exhibit ductile fracture. Obvious extrusion mark (arrow direction in Fig. 6 (a)) on the surface can be observed in PAN fibers, while the surface of the PAN/CNT-COOH fibers becomes smoother. It is suggested that [15] the CNTs at the skin of the fibers modify their interaction with the extrusion die, resulting in a smooth skin. The PAN/CNT-COOH fibers with 0.5 wt.% CNTs-COOH exhibit a fairly uniform dispersion of apparently single CNT within the PAN matrix, which is consistent well with the observation in optical micrographs.

The diameter of PAN/CNT-COOH fibers is similar to that of PAN fibers, confirming that the plasticizing effect is not affected as the CNTs-COOH are added. These results are in good agreement with the FTIR results.

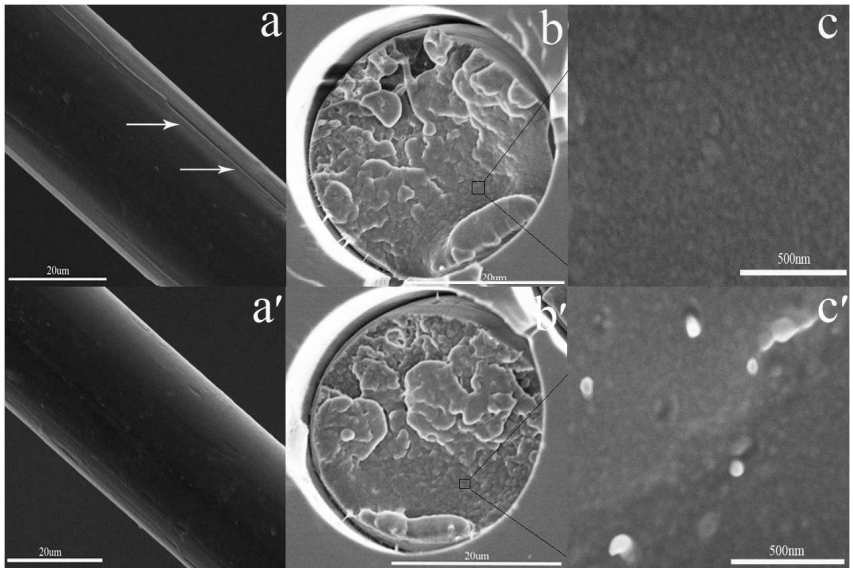

Fig. 6. The surface and cross-section of the PAN (a, b, c) and PAN/CNT-COOH (a′, b′, c′) fibers.

3.4 The mechanical properties of PAN and PAN/CNT-COOH composite fibers

Table 1 and Fig. 7 shows the mechanical properties of PAN and PAN/CNT-COOH composite fibers fabricated by plasticized spinning. The maximum tensile strength and initial modulus of PAN/CNT-COOH fibers are 0.475GPa and 10.93GPa, which are increased by 69.4% and 45.73% respectively compared with those of PAN fibers.

Interestingly, the elongation of PAN/CNT-COOH fibers with the CNTs-COOH content lower than 1wt.% is larger than that of PAN fibers, revealing that the strong inter-molecular interaction between C≡N groups is weakened as the CNTs-COOH are added. Therefore, PAN molecular chains are more likely to have a greater sliding motion, resulting in the increase in elongation. When the CNTs content exceeds 0.8wt.%, agglomeration is likely to take place in the fibers, this may destroy the orientation arrangement of PAN molecular chains, leading to the decrease in elongation.

The orientation in crystalline region also can be seen in Table 1, it can be observed that the PAN/CNT fibers exhibit a higher orientation than PAN fibers, revealing the addition of CNTs promotes the orientation of the fibers. The changing trend of orientation is consistent with tensile strength, indicating the orientation also improves the tensile strength of the fibers.

Table 1. Mechanical properties PAN, PAN/CNT and PAN/CNT-COOH fibers.

Sample	CNTs-COOH content (wt.% w.r.t PAN)	Spinning speed/m/min	Tensile strength /GPa	Tensile modulus /GPa	Strain to failure /%	Orientation/%
PAN fibers	-	48.8	0.2804	7.5	14.21	71.8
PAN/CNT-COOH fibers	0.5	49.2	0.378	7.84	14.64	73.2
	0.8	50	0.475	10.93	14.73	76.5
	1	49	0.424	8.43	12.96	74.7
	1.2	48.8	0.381	8.29	12.03	72.6

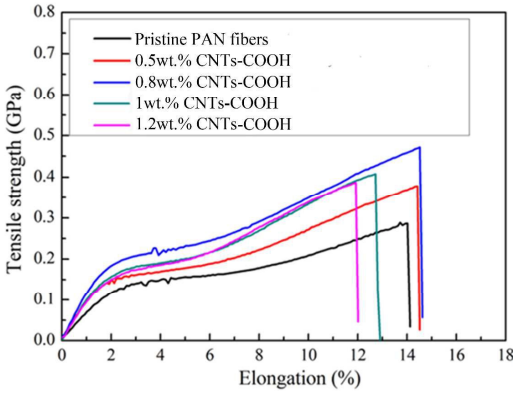

Fig. 7. The mechanical properties of the PAN and PAN/CNT-COOH fibers.

3.5 Surface chemical composition of PAN and PAN/CNT-COOH fibers

XPS was measured for PAN powder and fibers to confirm the chemical change during the plasticized spinning process. Table 2 shows the surface (5nm) atomic concentration of PAN and PAN/CNT-COOH fibers, the oxygen concentration in the surface of PAN powder is 2.93%, it is increased to 15.51% and 15.32% for PAN and PAN/CNT-COOH fibers, indicating the oxygen-containing groups are formed during the plasticized spinning process. The formed oxygen-containing groups can initiate the cyclization[16,35], meanwhile, the COOH groups in the CNTs-COOH also can initiate the cyclization[36]. Consequently, for the PAN/CNT-COOH fibers, the cyclization can be initiated by three types of initiating agents, i.e., carboxyl groups(-COOH) in CNTs, oxygen containing groups formed during the plasticized spinning and comonomers (methylacrylate and acrylamide) in PAN[20].

It is very interesting to note that the nitrogen concentration is reduced sharply for PAN and PAN/CNT-COOH fibers compared with PAN powder, especially the PAN fibers. This may be due to that there exist strong inter-molecular interaction between the C≡N groups in the surface and those in the inner induced by conformational changes from helical to planar zigzag (in Fig. 8), which can be further confirmed by XRD results in the later section. Lots of

C≡N groups in the surface are apt to arrange close to the center of fiber. Thus it is very hard to detect the C≡N groups in the surface. Meanwhile, the introduction of the CNTs-COOH to PAN weakens the inter-molecular interaction[15], especially the molecular chains at the amorphous region. It is speculated that partial C≡N groups in the surface would form "π-π" interaction with CNTs-COOH, but a large number of C≡N groups would not have obvious interaction with CNTs-COOH (in Fig. 8). As a result, these C≡N groups would arrange close to the surface of the fibers. Thus the PAN/CNT-COOH fibers exhibit higher nitrogen concentration in comparison with PAN fibers.

As shown in Fig. 9, the N_{1s} spectrum of the PAN powder shows a symmetrical peak at B.E. of 398.2 eV, which is assigned to C≡N groups. Partial C≡N groups of both fibers are converted to aromatic C=N groups due to the occurrence of cyclization during the plasticized spinning process, which can be proved by the appearance of a new peak at B.E. of 399.4 eV [37].

Table 2. Atomic concentration of surface of PAN and PAN/CNT-COOH fibers.

Sample	Atomic concentration (%)		
	C	O	N
PAN powder	79.81	2.93	17.27
PAN fibers	82.67	15.51	1.81
PAN/CNT-COOH fibers	81.12	15.32	3.56

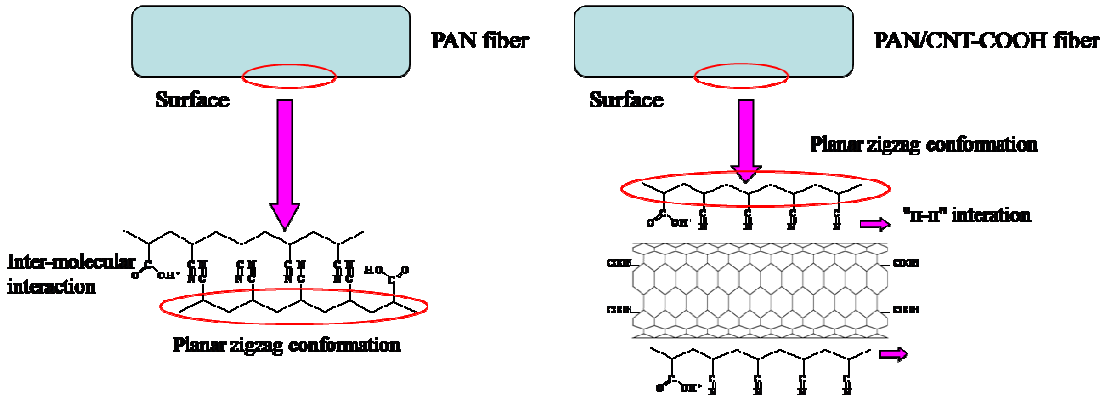

Fig. 8 The possible arrangement of C≡N groups in the surface of the fibers.

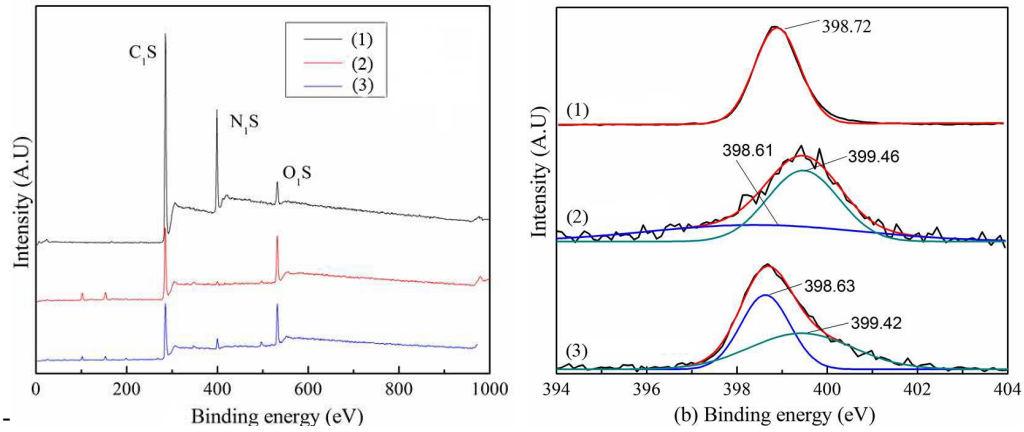

Fig. 9. XPS spectra of PAN powder, PAN and PAN/CNT-COOH fibers: (1) PAN powder, (2) PAN fibers (3) PAN-COOH fibers.

3.6 Crystallization and cyclization behaviors of PAN/CNT-COOH fibers

As can be seen in Table 2, with increasing the spinning speed, the crystallinity of the fibers is decreased at first then increased. The fibers with high CNTs-COOH content exhibit high crystallinity (similar spinning speed), indicating the introduction of CNTs-COOH contributes to crystallization. The initiation temperature for cyclization (T_i) is gradually decreased, cyclization temperature for cyclization (T) exhibits a identical changing trend compared with crystallinity, but the heat released (ΔH) for cyclization shows a opposite changing trend.

The changing trend of crystallinity may be associated with oriented-crystallization of PAN molecular chains and the heat exchange of the PAN/PL/COOH-CNT system during the plasticized spinning. High oriented-crystallization rate contributes to the crystallinity, but high heat exchange rate induced by high thermal conductivity of CNTs [38,39] is not conducive to the crystallinity since it shortens the oriented-crystallization stage. Consequently, these two factors have opposite effects on crystallinity. It is noted that the

oriented-crystallization rate and heat exchange rate are both increased with increasing spinning speed, thus the changing trend in crystallinity of the resulting fibers is strongly dependent on spinning speed.

That is to say, the decrease in crystallinity of the fibers indicates that the high exchange rate of the system plays a decisive role at this spinning speed. As the spinning speed is further increased, high oriented-crystallization rate is considered to be the prime reason for the increase in crystallinity. Table 2 also shows that the crystal size (1.1-1.32nm) of all fibers prepared by plasticized spinning are obvious smaller than that (3.7-5nm) of and PAN/CNT-COOH fibers fabricated by wet-spinning [9], this can be explained by high spinning speed for plasticized spinning, which hinders the growth of the crystal.

Table 2. The Structural parameters of PAN/CNT-COOH fibers.

CNTs-COOH content (wt.% w.r.t PAN)	Spinning speed/m/min	Crystallinity/%	Crystal size/nm	Meridional peak position (2θ)/º
0.5	30.3	56.1	1.2	40.68
	40.2	54.2	1.13	40.33
	49.2	65.2	1.24	40.62
0.8	30	63.26	1.25	40.62
	40.1	61.04	1.12	40.15
	50	68	1.31	40.55

Fig.10 shows the XRD curves of the PAN/CNT-COOH fibers, where the peak position at round 36º and 40º are ascribed to planar zigzag and helical sequences respectively[40]. Thus Peakfit soft (v4.12) was utilized for peak fitting of XRD spectra in the range of 20°-50° and peak position (around 40º) was accurately calculated, as shown in Fig (a), Fig (a′) , Fig (b) and Fig (b′). The shift of peak position at round 40º to the low angle indicates the increase in planar zigzag conformation[10]. In this paper, the peak position (around 40º) of both fibers is shifted to low angle at first, and then shifted to high angle, which is in agreement with the

crystallinity. This may reveal that the high spinning speed contributes to conformational changes from helical to planar zigzag and conformational changes are apt to take place at amorphous region other than crystallinity region. In this case, the fibers with higher CNTs-COOH content (similar spinning speed) possess more planar zigzag conformation, indicating the addition of CNTs-COOH is conducive to conformational changes.

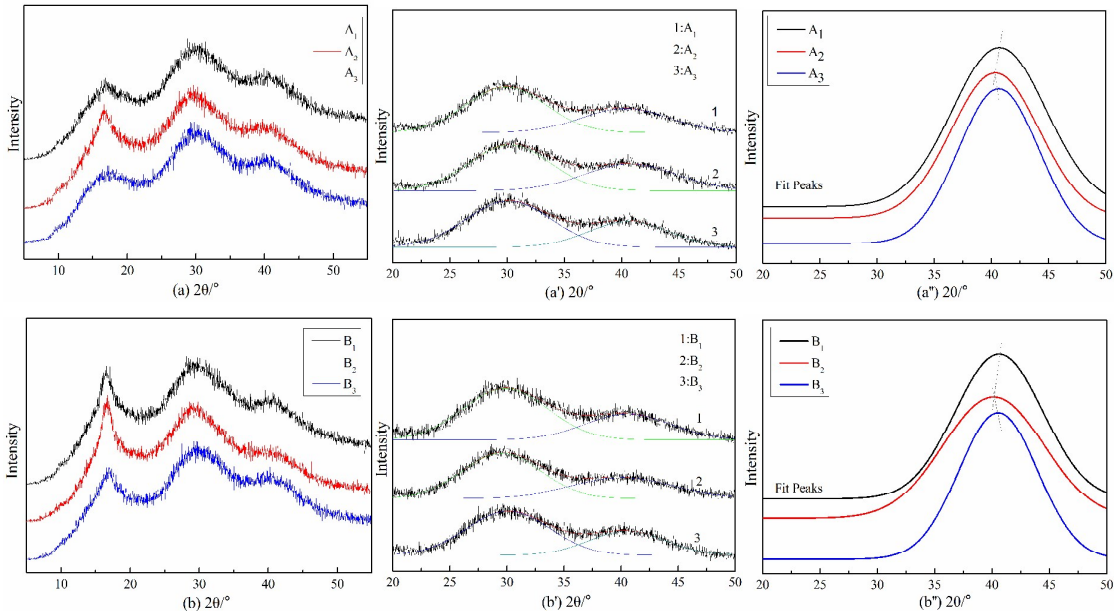

Fig. 10. XRD meridional scans of PAN/CNT-COOH fibers: (a) 5-55°, (a′) and (a′′) 0.5wt.% CNTs; (b), (b′) and (b′′) 0.8wt% CNTs; A_1: 30.3m/min, A_2: 40.2m/min, A_3: 49.2m/min, B_1: 30m/min, B_2: 40.1m/min, B_2: 50m/min.

Cyclization reaction first occurs at amorphous region, then propagates to crystalline region [41,42], consequently, the T_i reflects the cyclization at amorphous region. As mentioned before, the addition of CNTs-COOH to the PAN results in the formation of the "π-π" interaction between PAN and CNTs-COOH (confirmed by FTIR), which would weaken the intermolecular interaction between C≡N groups of the fibers at amorphous region. Furthermore, high spinning speed may leads to conformational changes of PAN molecular chains from the helical to planar zigzag (confirmed by XRD results), which raises the possibility of interaction between PAN molecular chains and CNTs-COOH. Consequently, it

is reasonable to conclude that the intra-molecular cyclization [43] becomes easier to take place at amorphous region, resulting in the decrease in the T_i (in Table 3 and Fig. 11). It is interesting to note that the fibers with 0.8wt.% CNTs-COOH show a lower T_i (in Table 3 and Fig. 11) compared with the ones with 0.5wt.% CNTs-COOH (similar spinning speed), suggesting that the CNTs-COOH, like common acids [44], can lower the T_i.

The ΔH (in Table 3) is increased at first, and then decreased. As mentioned before, the high spinning may contributes to conformational changes of PAN molecular chains from helical to planar zigzag, which facilitates the cyclization [17]. In this case, the fibers possess more planar zigzag conformation exhibit higher ΔH, which is consistent with the XRD results.

Table 3. The DSC data of PAN/CNT-COOH fibers in the range of 200ºC-380ºC.

CNTs-COOH content (wt.% w.r.t PAN)	Spinning speed/m/min	T_i/ºC	T/ºC	ΔH /Jg^{-1}
0.5	30.3	239	266.2	480.2
	40.2	237.13	265.17	572.9
	49.2	235.62	267.66	517.2
0.8	30	237.26	268.17	447.6
	40.1	235.44	266.76	525.2
	50	235.01	268.3	491.6

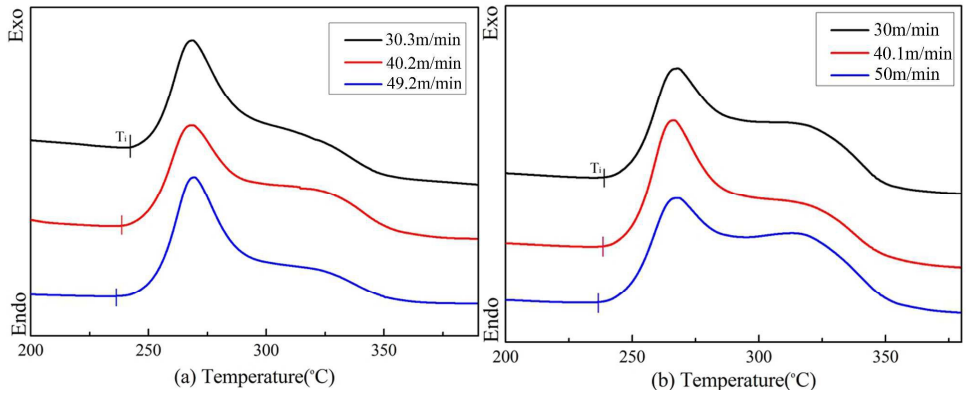

Fig. 11. The DSC curves of the PAN/CNT-COOH fibers: (a) 0.5wt.% CNTs-COOH content, (b) 0.8wt.% CNTs-COOH content.

The fibers containing 0.5wt.% CNTs-COOH show a higher ΔH compared with the ones

containing 0.8wt.% CNTs-COOH (similar spinning speed). In order to prove the effect of the CNTs-COOH, the fibers with spinning speed of 30.3m/min (0.5wt.%) and 30m/min (0.8wt.%) were used for measurement. These fibers were heated again to 400°C at the heat rate of 10m/min after the first heating, the results can be seen in Fig.12. No exothermic peak can be observed for both fibers, indicating the vast majority of C≡N groups are involved in the cyclization as the fibers were heated for the first time. This further reveals that the introduction of CNTs-COOH, just like comonomer[20], can reduce the ΔH for cyclization. Thus, the fibers containing a higher CNTs-COOH content exhibit a lower ΔH.

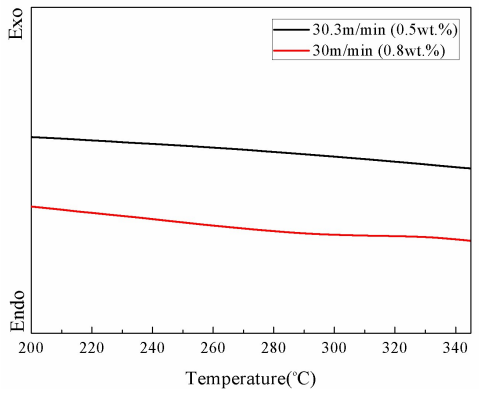

Fig. 12. The DSC curves of both fibers after heating again.

4. Conclusion

[Bmim]Cl was utilized as a plasticizer to achieve the plasticized spinning of PAN and PAN/CNT-COOH composite fibers. It is observed that the CNTs-COOH dispersed well in the PAN/CNT-COOH fibers. The results show that the plasticizing effect of the PAN/PL/CNT-COOH system is not affected as the the CNTs-COOH are added.

The maximum tensile strength and initial modulus of PAN/CNT-COOH fibers were 0.475GPa and 10.93GPa, which were increased by 69.4% and 45.73% respectively as compared with the PAN fibers. The crystallinity of PAN/CNT-COOH is decreased with

increasing the spinning speed, and then increased, which is associated with the high heat exchange rate and high oriented-crystallization. The cyclization of the fibers was initiated by three types of initiating agents. The T_i of PAN/CNT-COOH fibers is decreased with increasing spinning speed and higher CNT-COOH content contributes to initiation of cyclization. The fibers possess more planar zigzag conformation exhibit higher ΔH, suggesting the increase in planar zigzag conformation facilitates the cyclization.

Notes and references

[1] M. C. Paiva, C. A. Bernardo and M. Nardin, Carbon, 2000, 38, 1323.
[2] M. Y. Wu, Q. Y. Wang, K. N. Li, Y. Q. Wu and H. Q. Liu, Polym. Degrad. Stab., 2012, 97, 1511.
[3] M. S. A. Rahaman, A.F. Ismail and A. Mustafa, Polym. Degrad. Stab., 92, 1421.
[4] H. L. Zhang, L. H. Xu, F. Y. Yang and L. Geng, Carbon, 2010, 48, 688.
[5] H. G. Chae, M. L. Minus and S. Kumar, Polymer, 2006, 47, 3494.
[6] H. Zhou, X. Y. Tang, Y. M. Dong, L. F. Chen, L.T. Zhang, W. R. Wang and X. P. Xiong, J. Appl. Polym. Sci., 120, 1385.
[7] H. G. Chae, M. L. Minus, A. Rasheed and S. Kumar, Polymer, 2007, 48, 3781.
[8] A.T. Chien, P. V. Gulgunje, H. G. Chae, A. S. Joshi, J. Moon, B. Feng, G. P. Peterson and S. Kumar, Polymer, 2013, 54, 6210.
[9] H. G. Chae, T. V. Sreekumar, T. Uchida and S. Kumar, Polymer, 2005, 46, 10925.
[10] H. G. Chae, M. L. Minus and S. Kumar, Polymer, 2006, 47, 3494.
[11] R. Jain, H. G. Chae and S. Kumar, Compos. Sci. Technol., 2013, 88, 134.
[12] S.K. Atureliya and Z. Bashir, Polymer, 1993, 34, 5116.
[13] B.G. Min and C.W. Kim, j. appl. polym. sci., 2001, 84, 2505.
[14] L. Vaisman, E. Wachtel, H. D. Wagner and G. Marom, Polymer, 2007, 48, 6843.
[15] L. Vaisman, B. Larin, I. Davidi, E. Wachtel, G. Marom and D. W. Wagner, Composites: Part A, 2007, 38, 1354.
[16] X. Li, A. W. Qin, X. Z. Zhao, B. M. Ma and C. J. He, Polymer, 2014, 55, 5773.
[17] O. K. Park, S. H. Lee, H. L. Joh, J. K. Kim, P. H. Kang, J. H. Lee and B. C. Ku. Polymer, 2012, 53, 2168.
[18] J. Zhang, Y. W. Zhang, D. G. Zhang and J. X. Zhao, J. Appl. Polym. Sci., 2011, 125, E58.
[19] Y. D., H. G. Chae and S. Kumar, Carbon, 2011, 49, 4477.
[20] P. Bajaj, T. V. Sreekumar and K. Sen, Polymer, 2001, 42, 1707.
[21] M. C. Paiva, P. Kotasthane, D. D. Edie and A. A. Ogale, Carbon, 2005, 43, 1399.
[22] P. Rangarajan, J. Yang, V. Bhanu, D. Godshall, J. Mcgrath, G. Wilkes and D. J. Baird, J. Appl.Polym.Sci. 2001, 85, 69.
[23] P. H. Wang, J. Liu, Z.R. Yue and R. Y. Li, Carbon, 1992, 30, 113.
[24] Y. D. Liu, H. G. Chae and S. Kumar, Carbon, 2011, 49, 4487.
[25] H. You, X. Li, Y. Yang, B. Y. Wang, Z. X. Li, X. F. Wang, M. F. Zhu and B. S. Hsiao. Sep. Purif.

Technol. , 2013, 108, 143..
[26] V. B. Gupta and S. Kumar. J. Appl. Polym. Sci. , 1981, 26, 1865.
[27] A. K. Gupta and R. P. Singhal, J. Polymer Sci. Polymer Phys.Ed. , 1983, 21, 2243.
[28] G. P. Wu, C. X. Lu, L. C. Ling, A. M. Hao and F. He, J. Appl. Polym. Sci., 2005, 96, 1029.
[29] H. Y. Zhao, S. Qiu, L, G, Wu, L. Zhang, H. L. Chen and C. J. Gao, J. Membr. Sci., 2014, 450, 249.
[30] R. Graupner, J. Raman Spectrosc., 2007, 38, 673.
[31] S. Rivera-Rubero and S. Baldelli, J. Phys. Chem. B, 2006, 110, 4756.
[32] Y. Jeon, J. Sung, D. Kim, C. Seo, H. Cheong, Y Ouchi, R. Ozawa and H. Hamaguchi, J. Phys. Chem. B, 2008, 112, 923.
[33] S. Bellayer, J. W. Gilman, N. Eidelman, S. Bourbigot, X. Flambard, D. M. Fox, H. C. De Long and P. C. Trulove, Adv. Funct. Mater, 2005, 15, 910.
[34] T. Fukushima, A. Kosaka, Y. Ishimura, T. Yamamoto, T Takigawa, N Ishii and T Aida, Science, 2003, 300, 2072.
[35] Y. D. Liu, H. G. Chae and S. Kumar, Carbon, 2011, 49, 4466.
[36] T. V. Sreekumar, L. Chandra, A. Srivastava and S. Kumar, Carbon, 2007, 45, 1114.
[37] R. J. J. Janson and H. Vabbekkum, Carbon, 1995, 33, 1021.
[38] S. Berber, Y. K. Kwon and D. Tomanek. Phys Rev Lett., 2000, 84, 4613.
[39] P. Kim, L. Shi, A. Majumdar and P. L. McEuen, Phys Rev Lett., 2001, 87, 215502-1.
[40] D. Sawai, A. Yamane, T. Kameda, T. Kanamoto, M. Ito, H. Yamazaki and K. Hisatani, Macromolecules, 1999, 32, 5622.
[41] A. Gupta and I. R. Harrison, Carbon, 1996, 34, 1427.
[42]A. Gupta and I. R. Harrison, Carbon, 1997, 35, 809.
[43] Y. D. Liu, H. G. Chae and S. Kumar, Carbon, 2011, 49, 4487.
[44] T. V. Sreekumar, L. Chandra, A. Srivastava and S. Kumar, Carbon, 2004, 45, 11050.

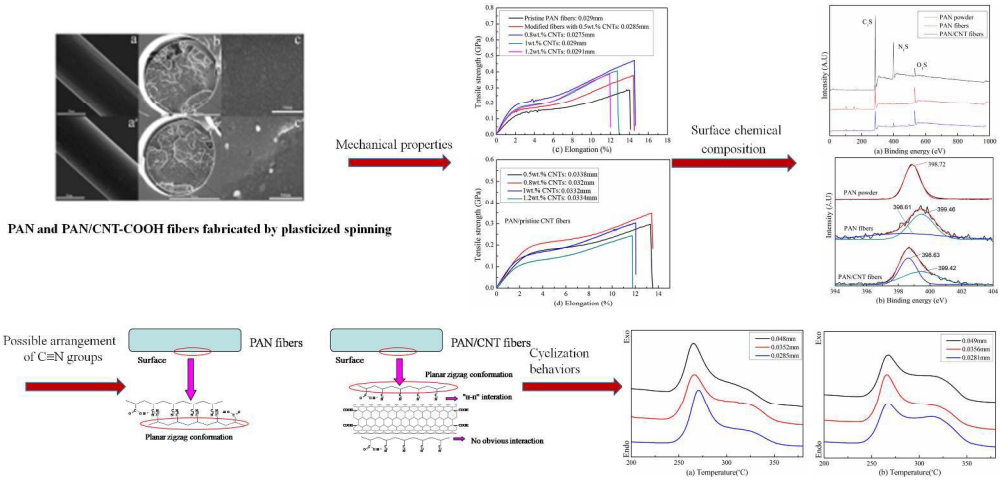

800x400mm (96 x 96 DPI)